Cyclic-Loading Performance of Steel Beam-to-Column Moment Connections to an I-Section Column

Martin SOMARRIBA
Candidate for the Degree of Master of Engineering
Supervisor: Dr. Taichiro Okazaki
Division of Architectural and Structural Design

Introduction

Although less commonly used than square-tube columns in Japanese steel construction, there are a significant number of low-rise buildings where I-section columns comprise moment resisting systems in both directions, in which case moment-resisting beam-to-column connections are placed to the column web as well as the column flange.

Limited research data is available in Japan for moment connections to I-section columns, whether to the column flange or column web. However, the current construction practice in Japan is very promising for steel beam-to-column moment connections because of the improvements in welding quality and in details like the non-weld access hole, which have been scarcely tested in connections to an I-section column.

Therefore, an experimental and analytical study was conducted primarily to fill the gap in knowledge due to the scarce experimental data on moment connections to an I-shaped column in Japan, and to examine the potential benefits that details of the Japanese construction practice on the seismic performance of these connections.

Literature Review

Most studies on beam-to-column moment connections to the flange and to the web of an I-section column were conducted in the United States prior to the 1994 Northridge earthquake.

Popov and Pinkney [1] observed that beam-to-column web connections are more prone to fracture than beam-to-column flange connections. A decade later, the monotonic-loading tests of beam-to-column web connections by Rentschler et al. [2] showed the importance of a strong connection of the beam web to the column. Tsai and Popov [3] used two vertical stiffeners to reinforce the continuity plates, and fillet welds to prevent slippage of the bolts in the web shear plate connection. The detail proved to reduce the strain concentrations in the continuity plates and substantially improved the cyclic-loading performance of the connection.

A post-Northridge research conducted by Gilton and Uang [4], indicated that the Reduced Beam Section (RBS) detail can reduce strain concentrations at the termination of the Complete Joint Penetration (CJP) groove welds to about one third compared to connections without RBS.

Research conducted in Japan by Nakagomi et al. [5] after the 1995 Kobe earthquake recommended the non-weld access hole method of construction to improve deformation capacity.

Test Plan

Fig. 1 shows the test setup and the definition of positive load. The T-configuration of the specimen represented an external beam-to-column subassembly of two to four-story steel moment frame buildings in Japan. A hydraulic jack with a capacity of ± 2000 kN and ± 150 mm stroke was used to apply horizontal loading at the free beam end, subjecting the specimens to cyclic loading according to the protocol specified in Section K2 of AISC Seismic Provisions [6].

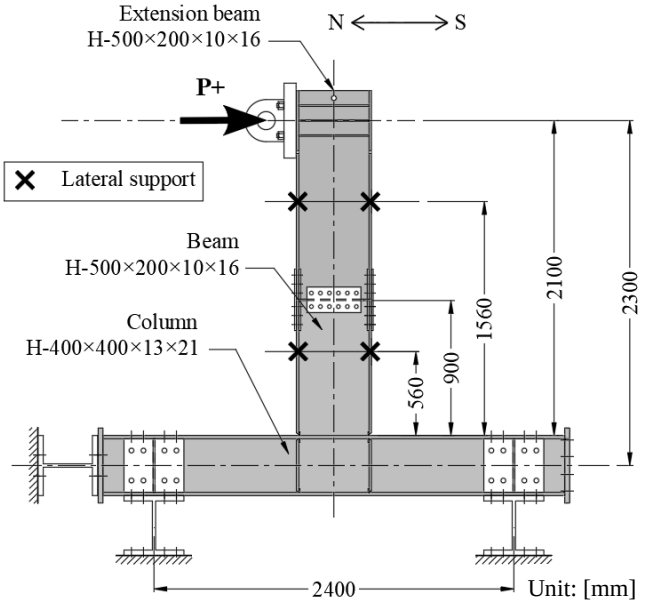

Fig. 1. Test setup

Fig. 2 shows the details of the six specimens: three for moment connection to the column flange (F1, F2 and F3) and three for moment connection to the column web (W1, W2 and W3). Complete Joint Penetration (CJP) groove welds were used to connect the beam flanges to the column: directly for F-specimens and through continuity plates for W-specimens. In both cases, the CJP welds were completed with no weld access holes.

Fillet welds were used to connect the beam web to the column: to the column flange for F-specimens, to the doubler plate for Specimen W2 and to the column web for Specimens W1 and W3. Specimen W2 was provided with a column doubler plate while Specimen W1and W3 were not, and Specimens W1 and W2 used a SN490C column with SN400B continuity plates while Specimen W3 a SN490B column with SN490B continuity plates.

A combination of displacement transducers and strain gages were used to measure the global and local responses of interest in this study.

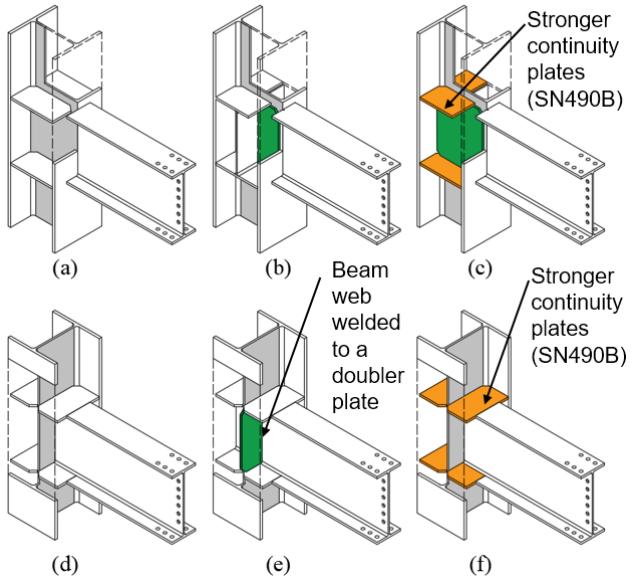

Fig. 2. Configuration of Specimen: a) F1, b) F2, c) F3, d) W1, e) W2, f) W3

Test Results

As shown in Figs. 3(a) and (b), the F-Specimens and Specimen W3 exhibited large local buckling deformation of the beam flanges and web. Prior to local buckling, cracks were detected in the groove weld joining the beam flanges to the column or the continuity plates. The cracks formed at the toe of the weld groove at the ends of the beam flange. In Specimen F1, the only F-Specimen without doubler plate, the cracks hardly grew. As shown in Fig. 3(c), the cracks in Specimens F2, F3 and W3 propagated straight along the weld groove, or the interface between the CJP groove weld and

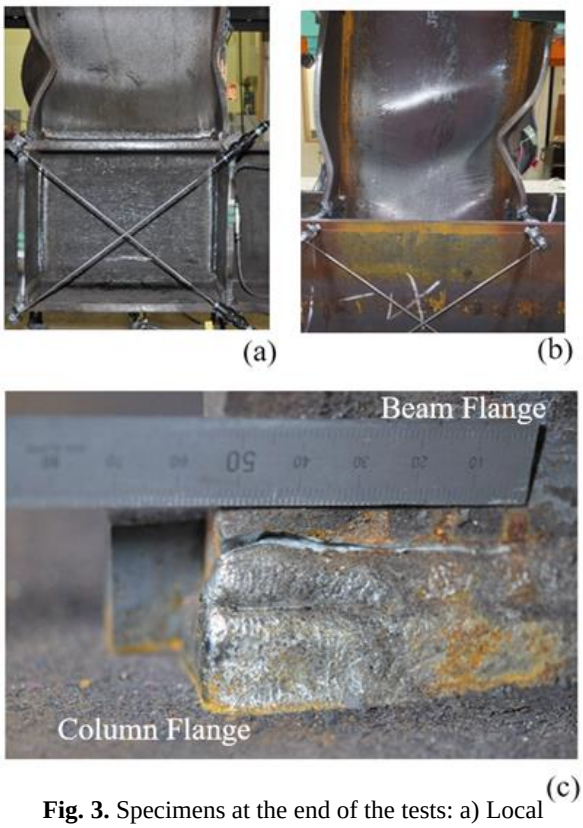

Fig. 3. Specimens at the end of the tests: a) Local buckling of F1; b) Local buckling of W3, and c) Crack at the groove weld termination of F2.

beam flange. Fracture initiating at the toe of the weld groove at the ends of the beam flange is a very typical failure mode for welded beam-to-column moment connections, particularly when the no weld access hole details is adopted [5]. Fig. 4 shows the measured moment at column face versus story drift ratio of the six specimens. From Fig. 4(a)–(c), the

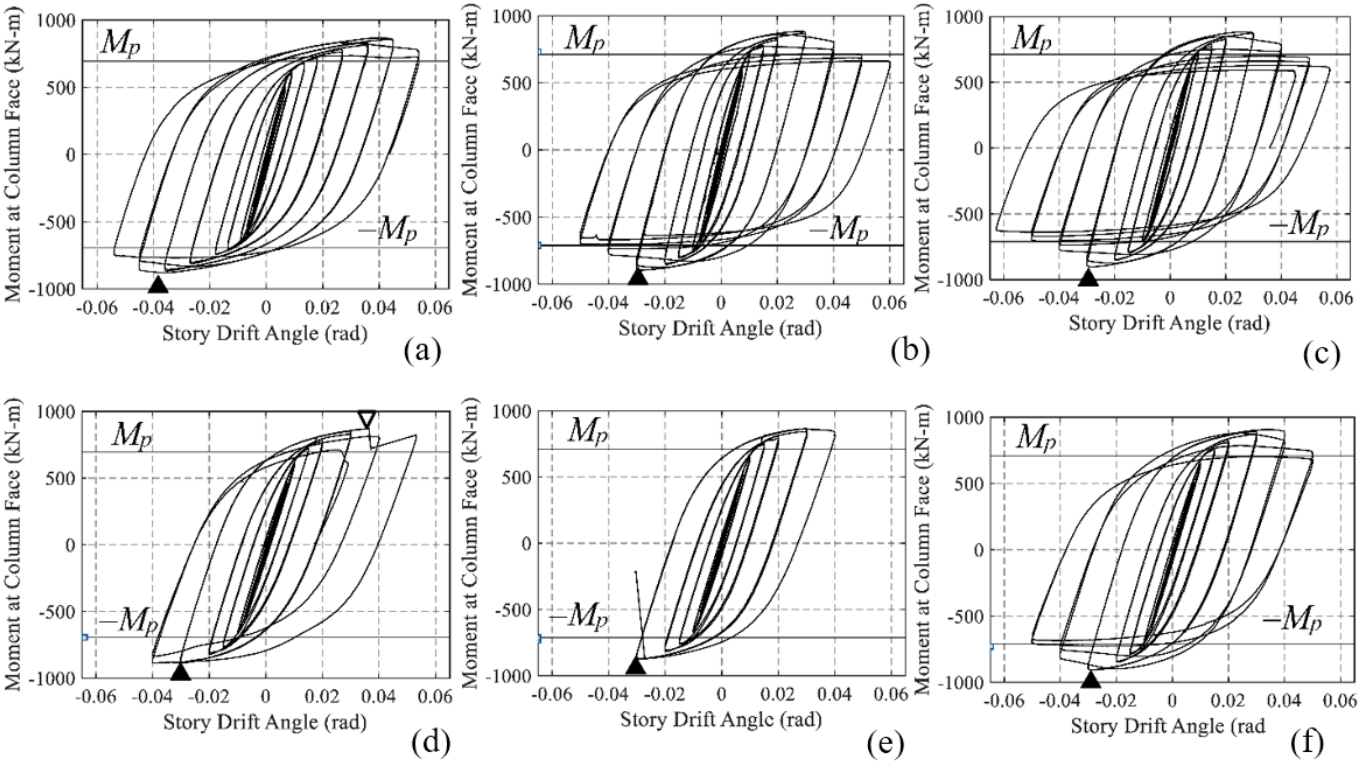

Fig. 4. Global response of Specimen: a) W1, b) W2, c) W3, d) F1, e) F2, f) F3

deformation capacity and strength of the F-Specimens was very similar.

Fig. 5. Fracture in the continuity plates of Specimens:

a) W1, and b) W2

The W-Specimens were prone to fracture of the continuity plate initiating at the termination of the beam flange groove weld, as shown in Fig. 5. Specimen W2 failed by sudden and complete fracture after that crack developed to about 20% of the width of the beam flange. Specimen W3 formed a very similar crack at the corner between the beam flange and continuity plate, but the cracks did not grow to a substantial size. Specimen W3 formed cracks along the groove of the beam flange, very much like the F-Specimens, which grew to a larger size than the cracks into the continuity plate.

Finite Element Analysis

Finite-element-method analysis of each tested specimen was performed using the general-purpose analysis software ADINA Ver.9.6 [7]. Fig. 6 shows the general features of the analysis model with the loading and boundary conditions.

Primary components were modeled with 3-D solid 8-node isoparametric elements with large displacement formulation and 2×2×2 Gauss integration points. The beam and column segments that were expected to remain elastic were modeled with 3-D 2-node beam elements. At the boundaries between solid elements and beam element, all degrees of freedom at the interface of solid section were slaved to the end node of the beam element. A combined translational and torsional spring provided lateral bracing to the beam at the points marked by "×" in Fig. 6.

Plastic-cyclic material model combining a bilinear isotropic model and two-term Armstrong Frederick kinematic hardening model was assigned to the 3-D solid elements. Table 1 summarizes the material parameters, calibrated against monotonic and cyclic coupon test data. The 2-node beam elements were linear elastic.

Table 1. Parameters for the material model

Material	Isotropic		Kinematic	
	σ_y	E_p	h_i	ζ_i
SN400B	195	70	h_1 = 30 000	ζ_1 = 300
SN490B	275	40	h_2 = 200	ζ_2 = 15
SN490C	295	70		

Initial imperfection was implemented by amplifying the first buckling mode shape, obtained from a Linear Buckling Analysis, to maximum out-of-straightness of 2.1 mm (1/1000 of the beam length). Cyclic loading was applied at the free end of the beam to introduce the same loading history used in the connection tests.

Fig. 7 shows the principal stresses near the critical regions of the connection, when the beam flange is subject to tension at the first excursion of the ±0.03-rad cycle. At this stage, marked by "▲" in Fig. 4(d) and (e), the cracks observed in Specimens W1 and W2 propagated rapidly into the continuity plates.

All three web-connection numerical models showed notably high stress at the corner between the beam flange and continuity plate, at the location where all three specimens formed a crack. It is also noted that the large principal stress acted perpendicular to the corner, to open any crack formed at this location, as reported for Specimens W1 and W2. Although little difference in stress distribution was confirmed between the three models, the maximum principal stress was higher in Model W2 (803 N/mm^2) than in Models W1 and W3 (772 and 770 N/mm^2, respectively).

Fig. 7 also shows that the principal stresses flow toward the center of the beam flange in major-axis moment connections to an I-section column. However, the maximum stresses all along the groove weld remain high.

Fig. 8 plots the effective plastic strain computed along line "A" in the continuity plate, 7.5 mm away from the termination of the beam flange at the first incursion of the ±0.03-rad cycles, the last loading amplitude before the formation of

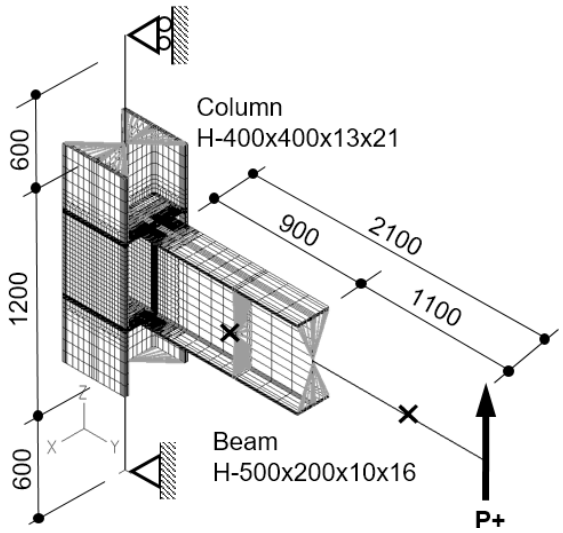

Fig. 6. Finite element model overview

cracks. Models W1 and W2, which were provided with a lower yield strength material (293 N/mm^2 opposed to 412 N/mm^2), experienced significantly larger plastic strains than Model W3 during these cycles. The variation was attributed to additional stresses induced to the continuity plates due to the presence or absence of column web doubler plate.

Discussion

The observed failure modes are regarded as the primary cause of strength reduction. Strength reduction was observed when crack propagation or excessive local buckling happened.

It is believed that the strength reduction caused by local buckling was the primary reason why these cracks did not propagate in the specimens examined in this program.

Specimens F2 and F3, whose panel zones were prevented from yielding, experienced larger crack growth compared to Specimen F1, which yielded in both the beam and panel zone.

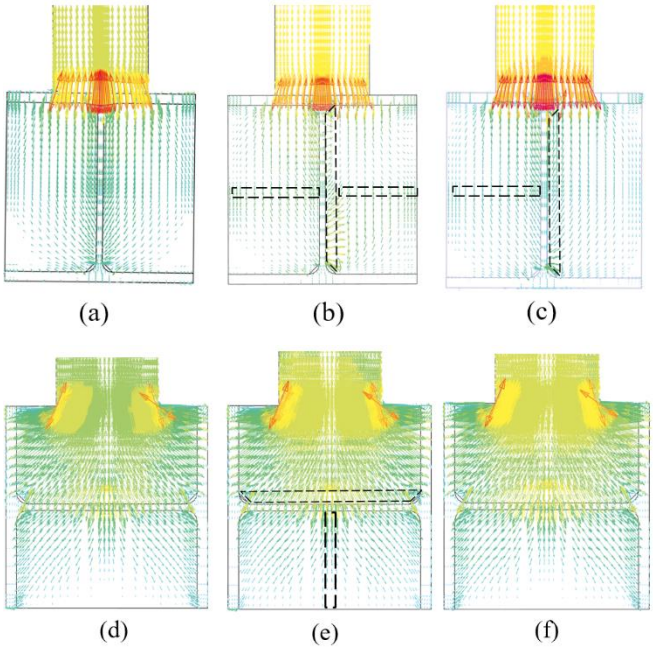

Fig. 7. Principal stress distribution at 0.03-rad story drift in Models: a) F1, b) F2, c) F3, d) W1, e) W2, and f) W3

Visual evidence during the tests and the comparison of plastic strains in Fig. 8 shows that the continuity plates in Specimen W2 yielded more significantly than in Specimen W3. During the tests, at ±0.02-rad and beyond, the strain at the sampled location grew much more substantially in Specimen W2, particularly in the diagonal direction to the beam axis. It is emphasized that the right corner between the beam flange and continuity plate, as well as cracks formed at this location, act as a notch placed perpendicular to such principal strain. The continuity plates were equal to the beam flanges in thickness. Therefore, it can be seen that the continuity plates in Specimens W1 and W2, which had lower yield strength than the beam flange (293 N/mm^2 compared to 321 N/mm^2) yielded while the continuity plates in Specimen W3, which had higher yield strength than the beam flange (412 N/mm^2 compared to 321 N/mm^2) did not yield as substantially. Consequently, the significantly different performance between Specimens W2 and W3 may be attributed to whether the continuity plates yielded during the test.

Conclusions

The main findings of this study are presented below:

- When brittle fracture of the continuity plates was avoided, the beam-to-column web connections were no less ductile than beam-to-column flange connections, and met the ductility requirements for SMFs per the AISC Seismic Provisions (AISC 2016).
- Beam-to-column web connections were prone to fracture of continuity plates initiating at the corner between the beam flange and the continuity plate. This failure mode was promoted by yielding of the continuity plates. Therefore, yielding of the continuity plates should be controlled by either adopting for the continuity plates a stronger material and/or thicker plate than the beam flanges.
- The shop-welded, no-access-hole detail for beam-to-column moment-resisting connections, which are commonly adopted in Japan, is a detail not included in ANSI/AISC 358-16 (AISC 2016) but met ductility requirements for SMFs per the AISC Seismic Provisions (AISC 2016).
- The observed behavior of Specimen W3 suggests that the quality of the welding process, in combination with having the beam web directly welded to the column web and the use of a stronger continuity plate were important factors to achieve a good seismic performance of the minor-axis moment connections even when continuity plates flush to the column flanges were used.

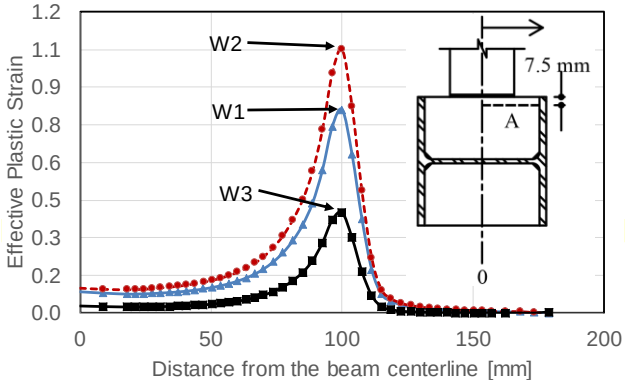

Fig. 8 Plastic strain distribution in the continuity plate of the W-Models at 0.03-rad story drift

Further research may address the aspects of actual buildings that were not considered in this study, such as the effect of composite action with the floor slab, the effect of bidirectional loading on the strength and stiffness of the connection, and varying the geometry of the continuity plate to avoid brittle fracture in connections to the column web.

References

[1] Popov, E. P., and Pinkney, R.B. *Behavior of steel building connections subjected to inelastic strain reversals*. Bull. No. 13, AISI, USA. 1968.

[2] Rentschler, G.P., Chen, W.-F., and Driscoll, G. C. Tests of beam-to-column web moment connections. Report No. 405.9, Fritz Engineering Laboratory. USA. 1978

[3] Tsai, K. C., and Popov, E. P. Steel beam-column joints in seismic moment resisting frames. Rep. No. UCB/EERC-88/19, EERC. Berkeley, CA: Univ. of California, Berkeley. 1988.

[4] Gilton, C. S., and Uang, C.-M. "Cyclic response and design recommendations of weak-axis Reduced Beam Section moment connections". *J. Struct. Eng*. 128 (4):452–463. 2002.

[5] Nakagomi, T., Fujita, T., Minami, K., Lee, K., and Murai, M. "Study on beam-end details for the method of non-scallop on beam-to-column welded joints." [In Japanese.] *J. Struct. Constr. Eng. Trans. AIJ* 62 (498), 145–151. 1997.

[6] AISC (American Institute of Steel Construction). Seismic Provisions for Structural Steel Buildings. ANSI/AISC 341-16. 2016.

[7] ADINA R&D, Inc. Theory and Modeling Guide. ADINA 9.6. 2020.